



Temperature-Stable High- ϵ Dielectrics Ceramics Based on $(1 - x)$ $\text{Ba}_5\text{NdTi}_3\text{Ta}_7\text{O}_{30}/x\text{Bi}_4\text{Ti}_3\text{O}_{12}$

X.H. ZHENG & X.M. CHEN*

Department of Materials Sciences & Engineering, Zhejiang University, Hangzhou (310027)

Submitted May 23, 2001; Revised January 23, 2003; Accepted January 23, 2003

Abstract. Modification of $\text{Ba}_5\text{NdTi}_3\text{Ta}_7\text{O}_{30}$ dielectric ceramics was investigated through introducing $\text{Bi}_4\text{Ti}_3\text{O}_{12}$. With increasing of $\text{Bi}_4\text{Ti}_3\text{O}_{12}$ content, the dielectric constant increased, and the temperature coefficient of the dielectric constant changed from negative to positive. The small temperature coefficient ($\tau_\epsilon < 50$ ppm/ $^\circ\text{C}$) combined with high dielectric constant ($\epsilon = 178$) and low dielectric loss ($\tan \delta = 0.007$ at 1 MHz) was achieved in the composition $x = 0.6$.

Keywords: dielectrics, temperature coefficient of dielectric constant, $\text{Ba}_5\text{NdTi}_3\text{Ta}_7\text{O}_{30}$, $\text{Bi}_4\text{Ti}_3\text{O}_{12}$, sintering

1. Introduction

With the rapid development in telecommunications and microelectronic technology, the dielectric ceramics have received much attention [1–3]. A high dielectric constant material can reduce the circuit dimension, and temperature stability of the dielectric properties is a necessary requirement for many applications such as mobile communication, automotive component and portable electronic devices. However, high dielectric constant materials typically have large temperature coefficients, and are often limited to dielectric constants to below 100. So far, the ceramics with perovskite structure has attracted most attention, while the ceramics with tungsten bronze structure have not been so extensively studied. Recently, tungsten bronze ceramics have attracted more and more scientific and commercial interests due to their many interesting properties, such as electric-optic, nonlinear, elasto-optic, acousto-optic, dielectric etc. [4–6].

Recently Chen et al. have proposed some promising candidates for high dielectric constant ($\epsilon > 100$) dielectric ceramics with tungsten bronze structure in the $\text{BaO-Nd}_2\text{O}_3\text{-TiO}_2\text{-Ta}_2\text{O}_5$ quaternary system [7–9]. In this system, $\text{Ba}_4\text{Nd}_2\text{Ti}_4\text{Ta}_6\text{O}_{30}$ has attracted much

attention due to its high dielectric constant ($\epsilon = 137$), and low dielectric loss ($\tan \delta = 0.0007$ at 1 MHz). $\text{Ba}_4\text{Nd}_2\text{Ti}_4\text{Ta}_6\text{O}_{30}$ ceramics has been modified through Bi, Sr and Ti substitutions for Nd, Ba and Ta respectively, and $\text{Ba}_4\text{Nd}_2\text{Ti}_4\text{Ta}_6\text{O}_{30}/(\text{La}_{0.9}\text{Bi}_{0.1})_2\text{Ti}_2\text{O}_7$ bi-phase system has also been investigated [10–13]. On the other hand, $\text{Ba}_5\text{NdTi}_3\text{Ta}_7\text{O}_{30}$ with larger negative temperature coefficient has not received enough attention, in spite of high dielectric constant and low dielectric loss. Meanwhile, it was reported that the layer structure compound $\text{Bi}_4\text{Ti}_3\text{O}_{12}$ had high dielectric constant of 180, and a large positive temperature coefficient of dielectric constant ($+650$ ppm/ $^\circ\text{C}$) [14, 15]. Several authors have reported the effects upon modifications of $\text{Ba}_{6-3x}\text{Nd}_{8+2x}\text{Ti}_{18}\text{O}_{54}$ ceramics through $\text{Bi}_4\text{Ti}_3\text{O}_{12}$ additions [16, 17].

In the present work, we attempt to create the temperature-stable dielectric ceramics by combining a negative temperature coefficient material $\text{Ba}_5\text{NdTi}_3\text{Ta}_7\text{O}_{30}$ with a positive temperature coefficient material $\text{Bi}_4\text{Ti}_3\text{O}_{12}$, and the influences of the sintering conditions upon the structures and properties are emphasized.

2. Experiments

All the samples were synthesized through a conventional solid-state reaction process with high-purity

*To whom all correspondence should be addressed. E-mail: xmchen@cmsce.zju.edu.cn

powders of BaCO_3 (>99.93%), Bi_2O_3 (>99%), Nd_2O_3 (>99%), TiO_2 (>99.8%) and Ta_2O_5 (>99.99%). The starting powders were weighed according to batch formula $(1-x)\text{Ba}_5\text{NdTi}_3\text{Ta}_7\text{O}_{30}/x\text{Bi}_4\text{Ti}_3\text{O}_{12}$, and ground in ethanol with ZrO_2 balls for 24 h. The powder mixtures were then dried and calcined at 800°C for one hour first in order to prevent Bi_2O_3 volatilizing, then heated to 1000°C for 3 h (1100°C for $x = 0.4, 0.45, 0.5$). The created powders were reground for one day and dried, then mixed with organic binder of 5 wt% polyvinyl alcohol (PVA). The powders were pressed into pellets with a cylindrical shape of 12 mm in diameter and 2 to 4 mm in thickness at a pressure of 98 MPa. The disks of $(1-x)\text{Ba}_5\text{NdTi}_3\text{Ta}_7\text{O}_{30}/x\text{Bi}_4\text{Ti}_3\text{O}_{12}$ were sintered well at the temperature range of 1100°C to 1200°C .

The bulk density of the sintered samples was measured by the dimensional method. The microstructures were characterized by the X-ray diffraction (XRD), using $\text{Cu K}\alpha$ radiation and scanning electron microscopy (SEM). The dielectric properties at room temperature were characterized by an LCR meter (HP4285A) from 100 KHz to 10 MHz. The temperature coefficient of the dielectric constant was measured at 10 KHz to 1 MHz by another LCR meter (HP4284A) equipped with a thermostat in the temperature range from room temperature to 85°C . Silver paste was used for the electrodes.

3. Results and Discussions

Compared with that of the end-member of $\text{Ba}_5\text{NdTi}_3\text{Ta}_7\text{O}_{30}$ [10–12], the densification temperature decreases by introducing $\text{Bi}_4\text{Ti}_3\text{O}_{12}$. As shown in Fig. 1, the present ceramics can be sintered to high density at the temperatures around 1150°C . The density of $(1-x)\text{Ba}_5\text{NdTi}_3\text{Ta}_7\text{O}_{30}/x\text{Bi}_4\text{Ti}_3\text{O}_{12}$ ceramics is slightly higher than that of $\text{Ba}_5\text{NdTi}_3\text{Ta}_7\text{O}_{30}$ ceramics.

XRD patterns of the present ceramics with various compositions are shown in Fig. 2. The phase constitutions and peak intensities obviously vary with the composition. The intensities of the peaks corresponding to $\text{Ba}_5\text{NdTi}_3\text{Ta}_7\text{O}_{30}$ tungsten bronze phase gradually decrease as x changes from 0.4 to 0.7, while the magnitude of the peaks for $\text{Bi}_4\text{Ti}_3\text{O}_{12}$ increases. The fraction of $\text{Bi}_4\text{Ti}_3\text{O}_{12}$ phase increases with increasing x , while that for $\text{Ba}_5\text{NdTi}_3\text{Ta}_7\text{O}_{30}$ phase decreases. However, the fraction of $\text{Bi}_4\text{Ti}_3\text{O}_{12}$ phase is obviously lower

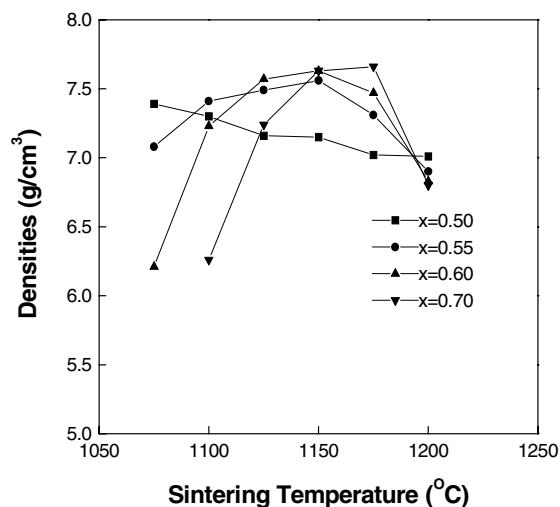


Fig. 1. Densities of $(1-x)\text{Ba}_5\text{NdTi}_3\text{Ta}_7\text{O}_{30}/x\text{Bi}_4\text{Ti}_3\text{O}_{12}$ ceramics versus sintering temperature.

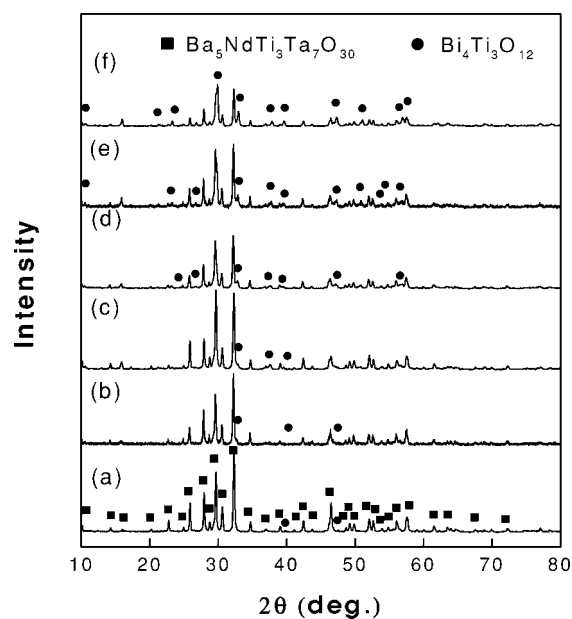


Fig. 2. XRD patterns of $(1-x)\text{Ba}_5\text{NdTi}_3\text{Ta}_7\text{O}_{30}/x\text{Bi}_4\text{Ti}_3\text{O}_{12}$ dielectric ceramics sintered at 1175°C in air for 3 h (a) $x = 0.40$, (b) $x = 0.45$, (c) $x = 0.50$, (d) $x = 0.55$, (e) $x = 0.60$ (sintered at 1150°C), and (f) $x = 0.70$.

than the nominal composition, and this suggests that $\text{Bi}_4\text{Ti}_3\text{O}_{12}$ partially dissolute into $\text{Ba}_5\text{NdTi}_3\text{Ta}_7\text{O}_{30}$ to form a solid solution with solubility less than 0.4.

SEM micrographs on the sintered surfaces of the present ceramics are shown in Fig. 3. Two kinds

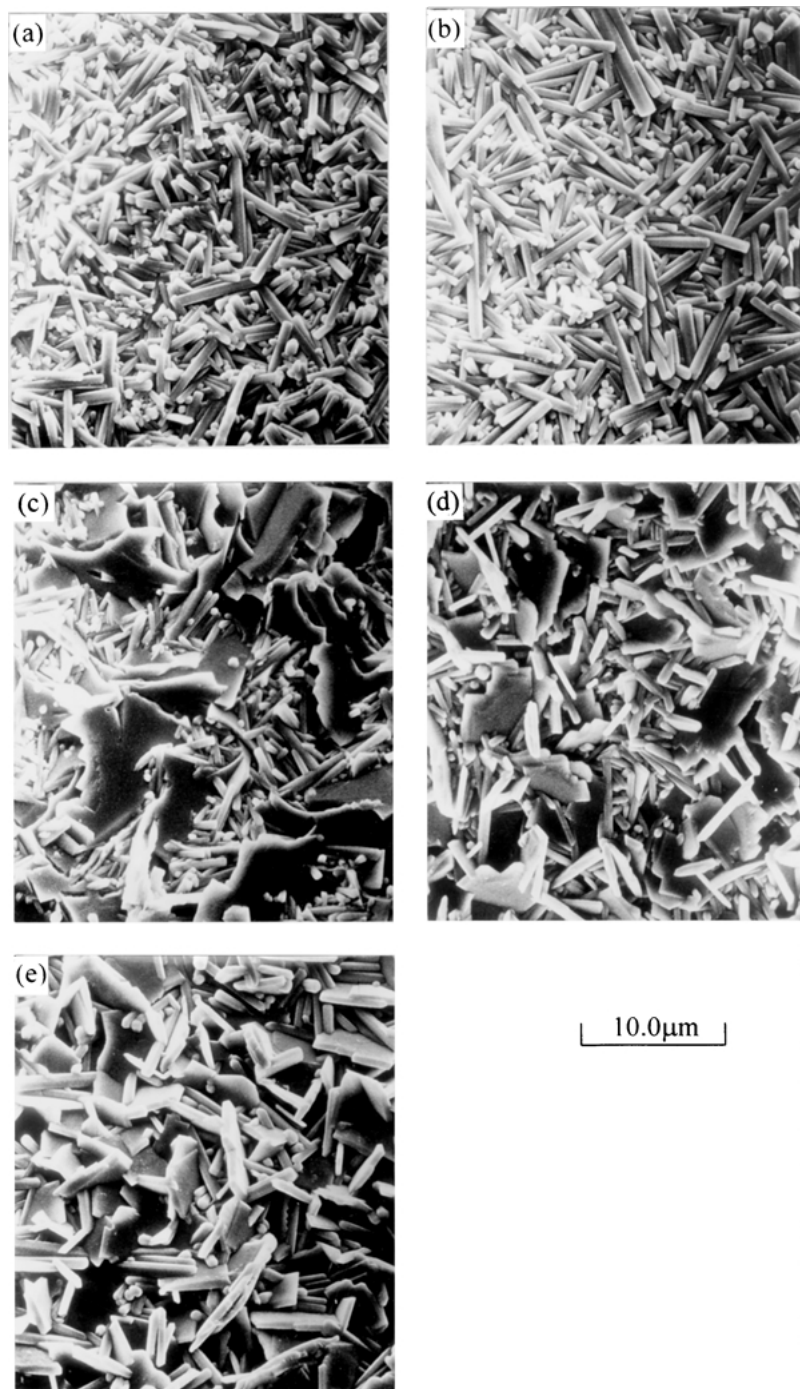


Fig. 3. SEM micrographs of $(1 - x) \text{Ba}_5\text{NdTi}_3\text{Ta}_7\text{O}_{30}/x\text{Bi}_4\text{Ti}_3\text{O}_{12}$ ceramics sintered at 1175°C in air for 3 h (a) $x = 0.45$, (b) $x = 0.50$, (c) $x = 0.55$, (d) $x = 0.60$ (sintered at 1150°C), and (e) $x = 0.70$.

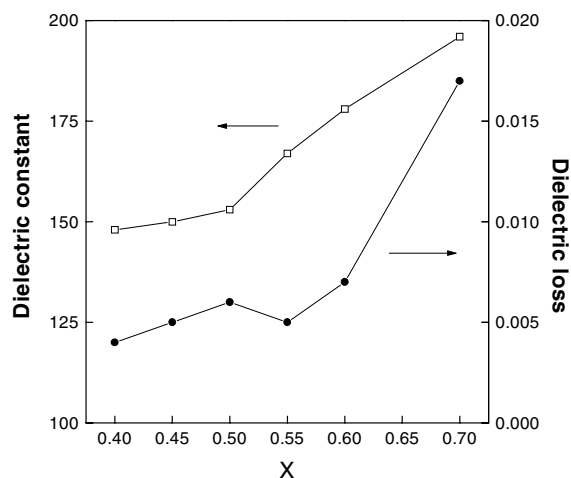


Fig. 4. Dielectric properties of $(1-x)\text{Ba}_5\text{NdTi}_3\text{Ta}_7\text{O}_{30}/x\text{Bi}_4\text{Ti}_3\text{O}_{12}$ ceramics as the functions of composition.

of grains with different morphologies, columnar and plate-like, are observed in the present ceramics. For $x = 0.55, 0.6$ and 0.7 , there are a few spherical grains, which suggest the present of some unknown phases. With increasing $\text{Bi}_4\text{Ti}_3\text{O}_{12}$ concentration, more plate-like grains are observed; this indicates that these plate-like grains belong to $\text{Bi}_4\text{Ti}_3\text{O}_{12}$ phase. Few plate-like grains disperse in the columnar matrix for $x \leq 0.5$, but the planar grains become dominate for $x > 0.6$. The results agree well with the analysis of XRD that $\text{Bi}_4\text{Ti}_3\text{O}_{12}$ and $\text{Ba}_5\text{NdTi}_3\text{Ta}_7\text{O}_{30}$ form partial solid solution.

Figure 4 shows the variation of dielectric constant and dielectric loss as the functions of the composition. With increasing the content of $\text{Bi}_4\text{Ti}_3\text{O}_{12}$, both dielectric constant and dielectric loss increase. When x is more than 0.6 , the dielectric loss of the present ceramics increases rapidly. These phenomena might concern with the space charge polarization of interfaces between the phases.

Figure 5 demonstrates the temperature coefficient of dielectric constant in the present ceramics as the function of $\text{Bi}_4\text{Ti}_3\text{O}_{12}$ content. With increasing $\text{Bi}_4\text{Ti}_3\text{O}_{12}$ content, the temperature coefficient of dielectric constant changes from negative to positive in the present ceramics, and it fails to agree with the models predicting dielectric behavior of mixture [18]:

$$\ln \varepsilon = V_1 \ln \varepsilon_1 + V_2 \ln \varepsilon_2 \quad (1)$$

$$\tau = V_1 \tau_1 + V_2 \tau_2 \quad (2)$$

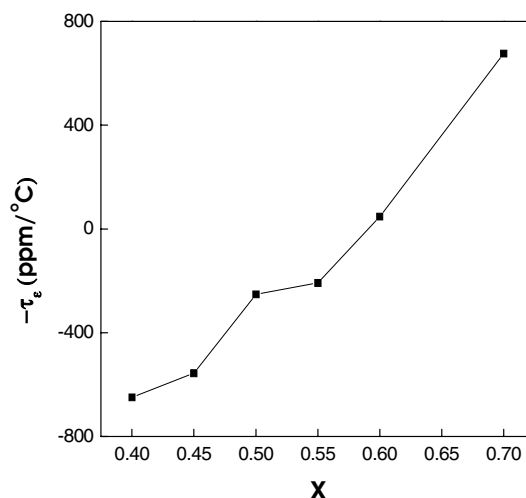


Fig. 5. Temperature coefficient of dielectric constant of $(1-x)\text{Ba}_5\text{NdTi}_3\text{Ta}_7\text{O}_{30}/x\text{Bi}_4\text{Ti}_3\text{O}_{12}$ ceramics as the function of composition.

where V_1 and V_2 are the volume fractions of the two components, ε_1 and ε_2 are their dielectric constants while ε is the resultant dielectric constant of the mixture, and τ_1 and τ_2 are the temperature coefficient for components. This may be due to the formation of a solid solution and production of unknown phase in the present ceramics. Meanwhile, the sintering condition has significant influence upon the dielectric properties of the present ceramics. A small temperature coefficient of the dielectric constant ($\tau_\varepsilon = 49$ ppm/°C) is obtained with high dielectric constant ($\varepsilon = 178$) and low dielectric loss ($\tan \delta = 0.007$) at 1 MHz for $x = 0.6$.

Figures 6 to 9 demonstrate that the sintering time has remarkable influences on the dielectric properties of the present ceramics with $x = 0.55$ and 0.6 . The dielectric loss for the present ceramics decreases with prolonging sintering except the case of $x = 0.55$ sintered for 2 h. This is originated from the increased homogeneity with increasing sintering time. Meanwhile, both the increased homogeneity and the volatilization of Bi lead to a decrease of dielectric constant with prolonging sintering. Dielectric constant of the present ceramics sintered for various time decreases with increasing frequency for $x = 0.55$, but it is almost a constant for $x = 0.6$. The dielectric loss decreases with increasing frequency for $x = 0.55$, while it increases linearly for $x = 0.6$.

As shown in Figs. 10 and 11, the sintering time has a strong influence on the temperature coefficient of

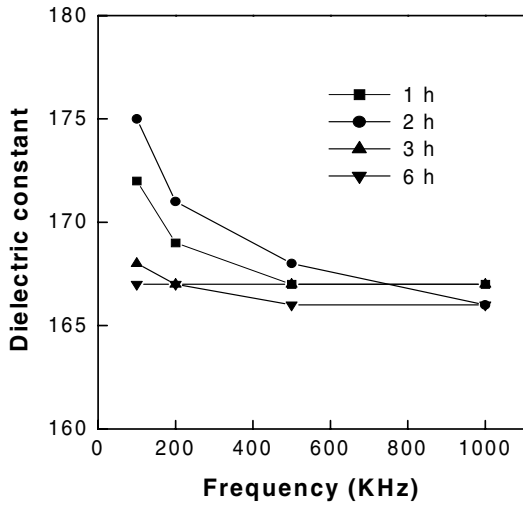


Fig. 6. Variation of dielectric constant of $(1 - x)$ $\text{Ba}_5\text{NdTi}_3\text{Ta}_7\text{O}_{30}/x\text{Bi}_4\text{Ti}_3\text{O}_{12}$ ($x = 0.55$) ceramics sintered at 1150°C with frequency and sintering time.

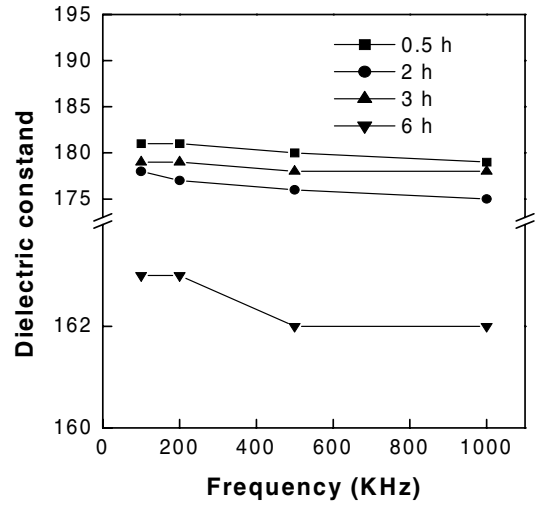


Fig. 8. Variation of dielectric constant of $(1 - x)$ $\text{Ba}_5\text{NdTi}_3\text{Ta}_7\text{O}_{30}/x\text{Bi}_4\text{Ti}_3\text{O}_{12}$ ($x = 0.6$) ceramics sintered at 1150°C with frequency and sintering time.

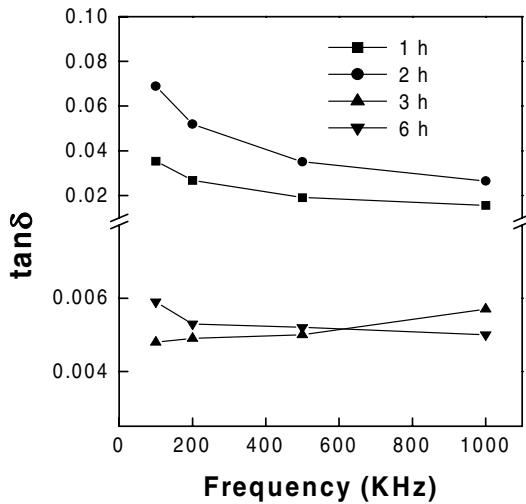


Fig. 7. Variation of dielectric loss of $(1 - x)$ $\text{Ba}_5\text{NdTi}_3\text{Ta}_7\text{O}_{30}/x\text{Bi}_4\text{Ti}_3\text{O}_{12}$ ($x = 0.55$) ceramics sintered at 1150°C with frequency and sintering time.

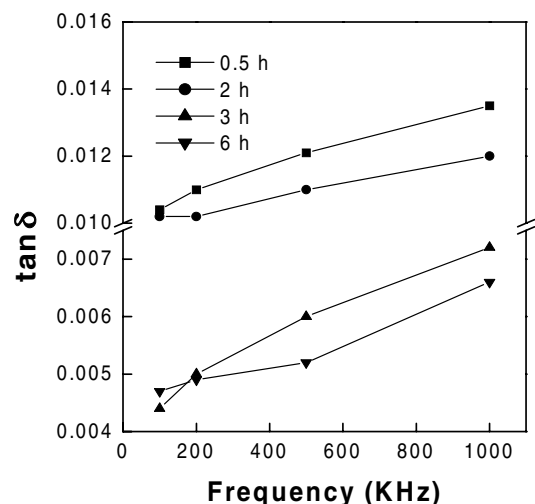


Fig. 9. Variation of dielectric loss of $(1 - x)$ $\text{Ba}_5\text{NdTi}_3\text{Ta}_7\text{O}_{30}/x\text{Bi}_4\text{Ti}_3\text{O}_{12}$ ($x = 0.6$) ceramics sintered at 1150°C with frequency and sintering time.

dielectric constant at various frequencies for the present ceramics with $x = 0.55$ and $x = 0.6$. For both compositions, the lowest temperature coefficients are obtained for a sintering time of 3 h. This is due to that the short time sintering inhibits the reactions and the formation of solid solution between $\text{Ba}_5\text{NdTi}_3\text{Ta}_7\text{O}_{30}$ and $\text{Bi}_4\text{Ti}_3\text{O}_{12}$, and the prolonged sintering accelerates these processes. The larger temperature

coefficients at lower frequencies well confirm these phenomena. That is, the inhomogeneities and the increased interfaces lead to the larger temperature coefficient at lower frequencies. In addition, it is interesting that the temperature coefficient of dielectric constant for $x = 0.55$ decreases with increasing frequency, while it increases for $x = 0.6$. This interesting phenomenon can be interpreted by the Debye

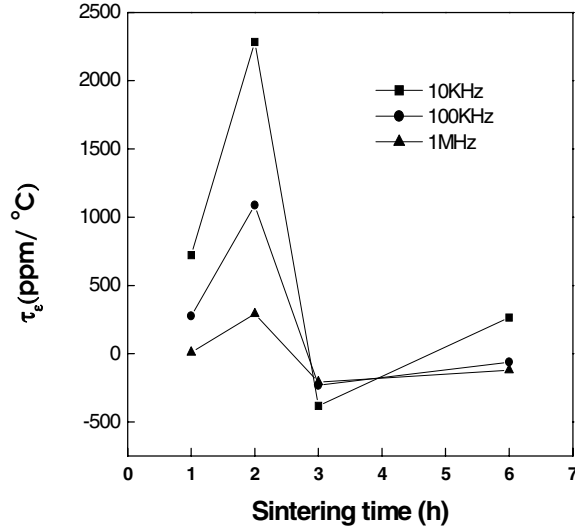


Fig. 10. Variation of temperature coefficient of dielectric constant of $(1-x)$ — $\text{Ba}_5\text{NdTi}_3\text{Ta}_7\text{O}_{30}/x\text{Bi}_4\text{Ti}_3\text{O}_{12}$ ($x = 0.55$) ceramics sintered at 1150°C with sintering time and frequency.

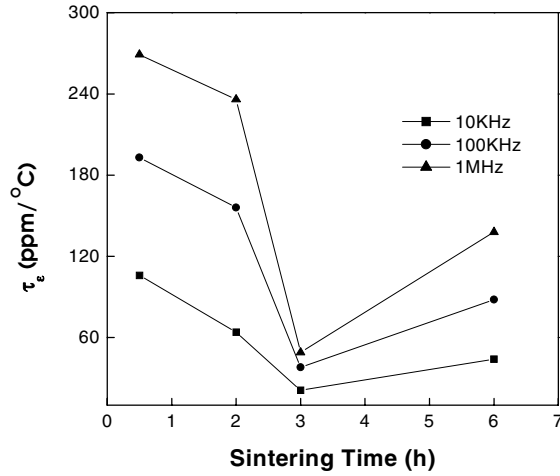


Fig. 11. Temperature coefficient of dielectric constant as functions of sintering time and frequency for $(1-x)$ $\text{Ba}_5\text{NdTi}_3\text{Ta}_7\text{O}_{30}/x\text{Bi}_4\text{Ti}_3\text{O}_{12}$ ($x = 0.60$) ceramics sintered at 1150°C .

equation [19]:

$$\varepsilon' = \varepsilon_\infty + \frac{\varepsilon_s - \varepsilon_\infty}{1 + \omega^2\tau^2} \quad (3)$$

$$\varepsilon'' = \frac{(\varepsilon_s - \varepsilon_\infty)\omega\tau}{1 + \omega^2\tau^2} \quad (4)$$

$$\tan \delta = \frac{\varepsilon''}{\varepsilon'} \quad (5)$$

where ε' and ε'' is the real and imaginary part of dielectric constant; ω , τ angular frequency and relaxation time, respectively, and $\tau = \tau_0 \exp(Q/KT)$ (τ_0 is a constant and Q is the activation energy of the 'dipole').

For $x = 0.55$, since the dielectric constant and dielectric loss decrease with increasing frequency, $\omega\tau/(1 + \omega^2\tau^2)$ decreases with increasing frequency according to Eqs. (3) to (5). Assuming $S = \omega\tau$, then

$$\frac{\partial\left(\frac{S}{1+S^2}\right)}{\partial S} = \frac{1-S^2}{(1+S^2)^2} < 0 \quad (6)$$

so infer that $S = \omega\tau > 1$. In addition,

$$\tau_\varepsilon = \frac{1}{\varepsilon} \frac{\partial \varepsilon}{\partial T} \frac{1}{\varepsilon} \frac{Z}{ZT} \quad (7)$$

So combining Eqs. (3) to (5) with above equation, we can deduce the following equations:

$$\frac{\partial \varepsilon}{\partial T} = \frac{(\varepsilon_s - \varepsilon_\infty)2\omega^2\tau}{(1 + \omega^2\tau^2)^2} \tau \frac{Q}{KT^2} \quad (8)$$

From Eqs. (3), (7) and (8), τ_ε can be written as:

$$\tau_\varepsilon = \frac{2\omega^2\tau^2 Q(\varepsilon_s - \varepsilon_\infty)}{KT^2(\varepsilon_s + \omega^2\tau^2\varepsilon_\infty)(1 + \omega^2\tau^2)^2} \quad (9)$$

Differentiating Eq. (9) with respect to frequency by considering parameters independence of frequency as a constant (positive), we can obtain:

$$\frac{\partial G}{\partial \omega} = \frac{4\omega\tau^2[\varepsilon_s(1 - \omega^2\tau^2) - 2\omega^4\tau^4\varepsilon_\infty]}{(\varepsilon_s + \omega^2\tau^2\varepsilon_\infty)^2(1 + \omega^2\tau^2)^3} \quad (10)$$

Where G presents $2\omega^2\tau^2/(\varepsilon_s + \omega^2\tau^2\varepsilon_\infty)(1 + \omega^2\tau^2)^2$. Since $S > 1$ (see Eq. (6)), we can conclude that $\frac{\partial \tau_\varepsilon}{\partial \omega} < 0$. In other word, the temperature coefficient of dielectric constant decreases with increasing frequency.

The similar deduction can be conducted for $x = 0.6$. In this case, $S = \omega\tau \ll 1$ can be obtained due to the dielectric constant keep almost a constant and dielectric loss increase with increasing frequency (as shown in Figs. 8 and 9), so Eq. (10) can be rewritten as

$$\frac{\partial G}{\partial \omega} = \frac{4\omega\tau^2(1 - \omega^2\tau^2)}{(1 + \omega^2\tau^2)^3} \quad (11)$$

Hence, the conclusion is $\frac{\partial \tau_\varepsilon}{\partial \omega} > 0$, then the temperature coefficient of dielectric constant increases with increasing frequency.

4. Conclusion

$\text{Ba}_5\text{NdTi}_3\text{Ta}_7\text{O}_{30}$ dielectric ceramics was modified by introducing $\text{Bi}_4\text{Ti}_3\text{O}_{12}$. The temperature-stable dielectric ceramics ($\tau_\epsilon = 49 \text{ pm}/^\circ\text{C}$) with high dielectric constant ($\epsilon = 178$) and low dielectric loss ($\tan \delta = 0.007$) were obtained $0.4\text{Ba}_5\text{NdTi}_3\text{Ta}_7\text{O}_{30}/0.6\text{Bi}_4\text{Ti}_3\text{O}_{12}$. Meanwhile, the effects of sintering process on the dielectric properties were studied, which affected the temperature coefficient significantly. And the analyses from theory on the effect were discussed. Temperature coefficients of the dielectric constant below $15 \text{ ppm}/^\circ\text{C}$ for $x = 0.55$ was achieved in the present ceramics sintered at 1150°C in air for 1 h or 9 h. Therefore, the present ceramics can be adjusted the dielectric properties through controlling the sintering process. These dielectric ceramics are promising in the applications such as high frequency capacitors and the temperature-compensated capacitors.

Acknowledgments

The present work was partially supported by Chinese National Key Project for Fundamental Researches under grant No. 2002CB613302, National Science Foundation for Distinguished Young Scholars under grant No. 50025205, and Chinese National Hi-Tech Project under grant number 2001AA325110.

References

1. S.L. Swartz, T.R. Shrout, and T. Takenaka, *Am. Ceram. Soc. Bull.*, **76**, 59 (1997).
2. G.H. Haertling, *J. Am. Ceram. Soc.*, **82**, 797 (1999).
3. R. Uvic, I.M. Reaney, and W.E. Lee, *Inter. Mater. Rev.*, **43**, 205 (1998).
4. R.R. Neurgaonkar and W.K. Cory, *J. Opt. Soc. Am.*, **3**(B), 276 (1986).
5. G.A. Rakuljic, K. Sayano, A. Yariv, and R.R. Neurgaonkar, *Appl. Phys. Lett.*, **50**, 10 (1987).
6. R.R. Neurgaonkar, W.F. Hall, J.R. Oliver, W.W. Ho, and W.K. Cory, *Ferroelectrics*, **87**, 167 (1988).
7. X.M. Chen and J.S. Yang, *J. Euro. Ceram. Soc.*, **19**, 139 (1999).
8. X.M. Chen, G.L. Lü, J.S. Yang, and Y.J. Wu, *J. Solid State Chem.*, **148**, 438 (1999).
9. X.M. Chen, J.S. Yang, and J. Wang, in *Dielectric Materials: Ceramic Transactions*, edited by K.M. Nair and A.S. Bhalla (The American Society, Westerville, OH, 1999), vol. 100, p. 71.
10. J. Wang, X.M. Chen, and J.S. Yang, *J. Mater. Sci. Mater. Elec.*, **10**, 483 (1999).
11. X.M. Chen, X.H. Zheng, and J. Wang, *J. Mater. Res.*, **16**, 2859 (2001).
12. X.H. Zheng and X.M. Chen, *Jpn. J. Appl. Phys.*, **40**, 4114 (2001).
13. J. Wang, X.M. Chen, and J.S. Yang, *J. Mater. Res.*, **14**, 3375 (1999).
14. E.C. Subbarao, *Phys. Rev.*, **122**, 804 (1961).
15. L.G. Van Uitert and L. Egerton, *J. Appl. Phys.*, **32**, 959 (1961).
16. Y.J. Wu and X.M. Chen, *J. Euro. Ceram. Soc.*, **19**, 1123 (1999).
17. D. Kolar, S. Gaberscek, Z. Stadler, and D. Suvorov, *Ferroelectrics*, **27**, 269 (1980).
18. A.E. Paladino, *J. Am. Ceram. Soc.*, **54**, 168 (1971).
19. P. Debye, *Polar Molecules* (New York, 1929).